HHS Public Access

Author manuscript

Nat Med. Author manuscript; available in PMC 2017 October 10.

Published in final edited form as:

Nat Med. 2017 May ; 23(5): 556–567. doi:10.1038/nm.4314.

Dectin-1 Activation on Macrophages by Galectin-9 Promotes Pancreatic Carcinoma and Peritumoral Immune-Tolerance

Donnele Daley[1,±], **Vishnu R. Mani**[1,±], **Navyatha Mohan**[1], **Neha Akkad**[1], **Atsuo Ochi**[1], **Daniel W. Heindel**[2], **Ki Buom Lee**[1], **Constantinos P. Zambirinis**[1], **Gautam S.D. Balasubramania Pandian**[1], **Shivraj Savadkar**[1], **Alejandro Torres-Hernandez**[1], **Shruti Nayak**[3], **Ding Wang**[4], **Mautin Hundeyin**[1], **Brian Diskin**[1], **Berk Aykut**[1], **Gregor Werba**[1], **Rocky M. Barilla**[1], **Robert Rodriguez**[1], **Steven Chang**[1], **Lawrence Gardner**[4], **Lara K. Mahal**[2], **Beatrix Ueberheide**[3], and **George Miller**[1,5,*]

[1]S.A. Localio Laboratory, Department of Surgery, New York University School of Medicine, 430 East 29th Street, New York, NY 10016

[2]Department of Chemistry, 100 Washington Square East, New York University, New York, NY 10003

[3]S.A. Localio Laboratory, Department of Biochemistry and Molecular Pharmacology, New York University School of Medicine, 430 East 29th Street, New York, NY 10016

[4]S.A. Localio Laboratory, Department of Medicine, New York University School of Medicine, 430 East 29th Street, New York, NY 10016

[5]S.A. Localio Laboratory, Department of Cell Biology, New York University School of Medicine, 430 East 29th Street, New York, NY 10016

Abstract

The progression of pancreatic oncogenesis requires immune-suppressive inflammation in cooperation with oncogenic mutations. However, the drivers of intra-tumoral immune tolerance are uncertain. Dectin-1 is an innate immune receptor critical in anti-fungal immunity, but its role in sterile inflammation and oncogenesis is not well-defined. Further, non-pathogen-derived ligands

Address correspondence to: George Miller, MD, Departments of Surgery and Cell Biology, New York University School of Medicine, 430 East 29th Street, East River Science Park, Room 660, New York, NY 10016, Tel: (646) 501-2208, Fax: (212) 263-6840, george.miller@nyumc.org.

[±]DD and VRM contributed equally to this work

Author Contributions

DD and VRM (project leadership, data collection and analysis, manuscript preparation), NM (flow cytometry, western blotting, invivo experiments, manuscript preparation), NA (IHC, IF, flow cytometry, invivo experiments), AO (immunoprecipitation, binding assays, ELISA, western blotting), KBL, GSDBP, SS and RR (flow cytometry, invivo experiments), DWH (immunoprecipitation and biochemical analysis), SN (mass spectroscopy), DW (cell line transfection), GW (invivo experiments), CPZ (data collection and mouse breeding), RMB, ATH, MH, BD and BA (technical assistance in diverse in vivo and in vitro experiments), SC (data analysis), LG (Cell line transfection), LKM (immunoprecipitation and biochemical analysis), BU (mass spectroscopy), GM (project design and leadership, data analysis, manuscript preparation).

Competing Financial Interests

The authors have competing interests.

GM - Co-Founder and Scientific Advisory Board Member of Nybo Therapeutics

for Dectin-1 have not been characterized. We found that Dectin-1 is highly expressed on macrophages in pancreatic ductal adenocarcinoma (PDA). Dectin-1 ligation accelerated PDA, whereas Dectin-1 deletion or blockade of its downstream signaling was protective. We found that Dectin-1 ligates the lectin Galectin-9 in the PDA tumor microenvironment resulting in tolerogenic macrophage programming and adaptive immune suppression. Upon interruption of the Dectin-1–Galectin-9 axis, $CD4^+$ and $CD8^+$ T cells – which are dispensable to PDA progression in hosts with an intact signaling axis – become reprogrammed into indispensable mediators of anti-tumor immunity. These data suggest that targeting Dectin-1 signaling is an attractive strategy for the immunotherapy of PDA.

Keywords

Pancreatic cancer; Kras; T cells; Myeloid-derived suppressor cells

Introduction

Pancreatic ductal adenocarcinoma (PDA) is a devastating disease with few long-term survivors[1]. Inflammation is paramount in PDA progression as oncogenic mutations alone, in the absence of concomitant inflammation, are insufficient for tumorigenesis[2]. Innate and adaptive immunity cooperate to promote tumor progression in PDA. In particular, specific innate immune subsets within the tumor microenvironment (TME) are apt at educating adaptive immune effector cells towards a tumor-permissive phenotype. Antigen presenting cell (APC) populations, including M2-polarized tumor-associated macrophages (TAMs) and myeloid dendritic cells (DC), induce the generation of immune suppressive Th2 cells in favor of tumor-protective Th1 cells[3,4]. Similarly, we and others have shown that myeloid derived suppressor cells (MDSC) negate anti-tumor $CD8^+$ cytotoxic T-Lymphocyte (CTL) responses in PDA and promote metastatic progression[5–7]. However, the drivers of monocytic cellular differentiation toward an immune-suppressive phenotype remain uncertain.

Dectin-1 is a member of the C-type lectin family of pattern recognition receptors and is expressed on the surface of macrophages and other cells of the myeloid-monocytic lineage[8]. Dectin-1 is a crucial component of the innate immune system's ability to recognize beta-glucan polysaccharides derived from fungal cell walls[9]. Ligation of Dectin-1 by β-glucans recruits the CARD9 adaptor protein, which phosphorylates Syk, thereby initiating an anti-fungal immune response[10,11]. Our recent work suggested that chronic inflammatory injury upregulates Dectin-1 expression in the liver[12]. Further, we found that the PDA TME is rife with damage associated molecular patterns (DAMPs) generated as byproducts of inflammation and necrotic cell death[3,13]. However, unlike Toll-like receptors, which influence oncogenic progression when ligated by DAMPs[3,14,15], the role of Dectin-1 in non-pathogen mediated inflammation or oncogenesis is not well-defined and sterile Dectin-1 ligands have not been characterized. We discovered high Dectin-1 expression and the presence of novel Dectin-1 agonists within the PDA TME. We postulated that Dectin-1 ligation in macrophages drives their immune suppressive cellular differentiation in PDA and thereby governs the tolerogenic T cell program in the TME which facilitates oncogenic progression.

Results

High Dectin-1 expression in murine and human PDA

To test the relevance of Dectin-1 signaling to pancreatic ductal adenocarcinoma (PDA), we examined Dectin-1 expression in two PDA mouse models: the slowly progressive PDA model $p48^{Cre}$;LSL-$Kras^{G12D}$ (KC) in which mice express oncogenic *Kras* in their pancreatic progenitor cells, and a more aggressive orthotopic PDA model utilizing tumor cells from $Pdx1^{Cre}$;LSL-$Kras^{G12D}$;$Tp53^{R172H}$ (KPC) mice, which expresses mutant *Kras* and *p53*; as well as in human PDA[42,43]. Immunohistochemical analysis suggested high Dectin-1 expression in leukocytes in KC pancreata and in transformed epithelial cells (Figures 1a and S1a, b). Pancreata from KC mice crossed with Dectin-$1^{-/-}$ animals (KC;Dectin-$1^{-/-}$) served as controls. Flow cytometry revealed ~2-fold higher Dectin-1 expression in macrophages (46%), neutrophils and inflammatory monocytes (80%), and DC (65%) within the KC TME compared with their cellular counterparts in spleen (18%, 47% and 40% respectively) (Figure 1b). Similarly, in orthotopically implanted KPC tumors, Dectin-1 was highly expressed on leukocytes and in malignant epithelial cells (Figures 1c and S1c–e). Dectin-1 was also expressed higher in leukocytes in PDA (44%) compared with normal pancreas (9%) (Figure 1d). Immune-fluorescent microscopy in human PDA similarly suggested high Dectin-1 expression in transformed epithelial cells and in tumor-infiltrating myeloid cells (Figure S1f, g). Parallel to mice, human PDA-infiltrating $CD14^+$ and $CD15^+$ monocytes and macrophages and $CD11c^+$ DC expressed higher Dectin-1 compared with their cellular counterparts in peripheral blood mononuclear cells (PBMC) (Figure 1e).

To investigate the stimulus for upregulation of Dectin-1 expression in leukocytes in PDA we co-cultured bone-marrow derived macrophages (BMDM) with pancreatic tumor cells derived from KPC mice. PDA cells and PDA cellular supernatant upregulated Dectin-1 expression in BMDM; however, select cytokines associated with PDA did not influence Dectin-1 expression (Figure S1h). Collectively, these results suggest upregulated Dectin-1 expression in the tumor and peritumoral inflammatory compartment in PDA.

Evidence of Dectin-1 signaling and the presence of Dectin-1 ligands in PDA

To investigate the relevance of Dectin-1 signaling in pancreatic oncogenesis, we assayed 3 and 6 month-old WT and KC pancreata for the presence of activated signaling intermediates downstream of Dectin-1 ligation. We found that compared with age-matched WT pancreata, KC pancreata expressed elevated p-Syk and p-PLCγ as well as high CARD9 and evidence of robust JNK pathway activation (Figure S2a). IHC confirmed high p-Syk expression in KC pancreata, whereas Syk signaling was reduced in PDA in the context of Dectin-1 deletion (Figure S2b). Similarly, flow cytometry showed elevated p-Syk expression in diverse myeloid cellular subsets in PDA compared with their counterparts in the spleen (Figure S2c).

To investigate for the presence of Dectin-1 ligands within the pancreatic TME, we employed a human IgG Fc-conjugated Dectin-1 fusion protein. Whereas Dectin-1 ligands were absent in WT pancreata, we identified high levels of Dectin-1 ligands in pancreata of KC mice by Western blotting (Figure S2a) and immune fluorescence microscopy (Figure S2d). Flow

cytometric analysis confirmed expression of Dectin-1 ligands on tumor-infiltrating macrophages and DC in KC pancreata compared with no expression in leukocytes in spleen (Figure S2e). Expression of Dectin-1 ligands were similarly elevated in APCs infiltrating orthotopic KPC tumors (Figure S2f). Further, $CD133^{+}$ transformed epithelial cells in KC (Figure S2g) and KPC tumors (Figure S2h) expressed Dectin-1 ligands *in vivo* as did KPC-derived tumor cells grown in culture (Figure S2i). Collectively, our data suggest high expression of the Dectin-1 receptor and Dectin-1 ligands in the epithelial and inflammatory compartments of PDA along with upregulation of associated signaling intermediates.

Dectin-1 ligation accelerates pancreatic oncogenesis

Since Dectin-1 and its cognate ligands are highly expressed in PDA, we postulated that Dectin-1 signaling may promote immune-suppressive inflammation leading to accelerated tumorigenesis. To test this, we serially treated six week-old KC mice with the Dectin-1 specific agonists depleted Zymosan (d-Zymosan) or Heat-killed Candida albicans (HKCA) and assessed tumor progression eight weeks later compared to vehicle-treated animals. Ligation of Dectin-1 vigorously accelerated tumorigenesis (Figure 1f–i). Whereas pancreata in vehicle-treated KC mice harbored large areas of residually normal acinar architecture, mice treated with Dectin-1 agonists exhibited near-complete effacement of their pancreatic acini with more advanced PanIN lesions and numerous foci of invasive carcinoma embedded in dense fibro-inflammatory stroma (Figure 1f–i). *Kras*-transformed ductal epithelial cells in Dectin-1 agonist-treated KC mice also exhibited elevated Ki67 proliferative rates (Figure S3a). Similarly, *in vivo* administration of Dectin-1 agonists accelerated tumor growth in orthotopically implanted KPC-derived tumors (Figure 1j). These data suggest that Dectin-1 signaling promotes PDA progression.

Dectin-1 deletion is protective against PDA

To determine whether Dectin-1 signaling is required for the normal progression of pancreatic oncogenesis, we examined the tumor-phenotype in KC;Dectin-$1^{-/-}$ mice over time. Dectin-1 deletion delayed malignant progression and stromal expansion. Compared with KC controls, age-matched KC;Dectin-$1^{-/-}$ pancreata exhibited delayed development of pancreatic dysplasia and fibrosis (Figures 2a, S3b) and extended survival (Figure 2b). To determine whether Dectin-1 deletion influences molecular oncogenesis, we probed pancreata from KC and KC;Dectin-$1^{-/-}$ mice for select cell cycle regulatory, oncogenic, and tumor suppressor genes. KC;Dectin-$1^{-/-}$ pancreata exhibited higher expression of Bcl-xL, Rb, Smad4, and p16 but reduced p53 and c-Myc expression suggesting a distinct oncogenic phenotype (Figure 2c). Collectively, these data imply that Dectin-1 contributes to the normal progression of pancreatic neoplasia in the context of a driving *Kras* mutation.

Syk inhibition is protective against PDA

Since Dectin-1 signals via Syk phosphorylation, and we showed that Syk activation is reduced in KC;Dectin-$1^{-/-}$ pancreata, we postulated that Syk blockade would be protective against pancreatic oncogenesis. KC mice were treated from 6–14 weeks of life with Piceatannol, a p-Syk inhibitor, and tested for tumor progression compared with vehicle-treated controls. We confirmed that Piceatannol prevented Syk activation *in vivo* in PDA. Syk inhibition reduced pancreatic tumor weights and mitigated dysplastic changes but was

not protective in KC;Dectin-1$^{-/-}$ mice (Figure 2d–e), suggesting that blockade of signaling pathways downstream of Dectin-1 may be an attractive therapeutic strategy in pancreatic oncogenesis.

Dectin-1 does not have direct pro-tumorigenic effects on transformed pancreatic ductal epithelial cells

To determine whether Dectin-1 ligation has direct mitogenic or activating effects on transformed pancreatic epithelial cells, we treated KPC-derived tumor cells *in vitro* with the Dectin-1 agonist d-Zymosan. Dectin-1 ligation failed to induce proliferation or cytokine production in PDA tumor cells (Figure S4a–c). HKCA similarly failed to induce proliferation or cytokine production in KPC cells (not shown). To further test whether Dectin-1 has direct oncogenic or pro-inflammatory effects in PDA cells, we silenced Dectin-1expression in KPC-derived tumor cells using shRNA (Figure S4d). However, Dectin-1 knockdown did not alter the growth rate of tumor cells *in vivo* (Figure S4e) suggesting that Dectin-1 signaling in the transformed epithelial compartment is not critical in modulating PDA. Similarly, transformed pancreatic ductal epithelial cells (PDEC) harvested from KC and KC;Dectin-1$^{-/-}$ pancreata proliferated at equal rates *in vitro* (Figure S4f) and *in vivo* (Figure S4g).

Dectin-1 deletion in the extra-epithelial compartment alone is protective against oncogenesis

Since Dectin-1 ligation or knockdown does not influence the proliferative capacity of transformed pancreatic epithelial cells, we postulated that Dectin-1 deletion in the extra-epithelial compartment alone would be protective against PDA. To investigate this, WT and Dectin-1$^{-/-}$ mice were challenged with orthotopic injections of KPC-derived tumor cells with intact Dectin-1 expression. Pancreatic tumors harvested at 3 weeks were markedly smaller in Dectin-1$^{-/-}$ hosts suggesting that Dectin-1 deletion in the extra-tumoral compartment alone is protective against PDA (Figure S4h). Dectin-1$^{-/-}$ mice also exhibited extended survival after orthotopic PDA tumor implantation compared with WT mice (Figure S4i). Similarly, KC mice made chimeric using Dectin-1$^{-/-}$ bone marrow were protected against oncogenesis compared with KC mice made chimeric using WT bone marrow, confirming that deletion of Dectin-1 in leukocytes alone is protective (Figure S4j). Dectin-1 expression was not associated with adverse survival in human PDA (Figure S4k); however, Dectin-1 was a surrogate for total myeloid cell infiltration (Figure S4l).

Dectin-1 deletion induces immunogenic reprogramming of tumor-infiltrating macrophages

We speculated that blockade of Dectin-1 signaling in the stroma leads to protection against PDA by bolstering anti-tumor immunity. Specifically, we postulated that Dectin-1 deletion leads to immunogenic reprogramming of macrophages resulting in the reversal of the immune-suppressive phenotype of PDA-infiltrating T cells. To test this *in vitro,* we stimulated naïve CD4^{+} and CD8^{+} T cells using CD3/CD28 co-ligation and measured expression of ICOS, CD44, IFN-γ, and TNF-α which are upregulated on activated T cells and expression of CD62L and IL-10 which is downregulated upon T cell activation. Dectin-1$^{+/+}$ or Dectin-1$^{-/-}$ CD11b^{+} cells harvested from KPC-derived tumors were added to select wells. Whereas tumor-infiltrating WT myeloid cells abrogated ICOS upregulation in

αCD3/CD28-activated $CD4^+$ and $CD8^+$ T cells, PDA-infiltrating Dectin-$1^{-/-}$ myeloid cells exhibited minimal inhibitory effects (Figure 3a, b). Similarly, whereas WT $CD11b^+$ cells prevented $CD4^+$ and $CD8^+$ T cell adoption of a $CD44^+CD62L^-$ effector memory phenotype in response to CD3/CD28 ligation, Dectin-$1^{-/-}$ cells were non-inhibitory (Figure 3c, d). Moreover, in contrast to tumor-infiltrating WT $CD11b^+$ cells which promoted IL-10 production from $CD4^+$ T cells (Figure 3e) and negated IFN-γ and TNF-α expression in $CD8^+$ T cells (Figure 3f), Dectin-$1^{-/-}$ cells only minimally induced IL-10 production in $CD4^+$ T cells and were permissive of $CD8^+$ cytotoxic T cell activation (Figure 3e, f). Similar differential effects on $CD4^+$ and $CD8^+$ T cell inhibition were observed when using purified $Gr1^-CD11c^-CD11b^+F4/80^+$ PDA-associated macrophages (TAMs) harvested from WT versus Dectin-$1^{-/-}$ hosts (Figure S5a, b). Conversely, the T cell inhibitory capacity of $Gr1^+CD11b^+$ neutrophils and inflammatory monocytes was not diminished in the context of Dectin-1 deletion suggesting that only Dectin-1 signaling in TAMs influences T cell function (Figure S5c).

To investigate whether Dectin-1 signaling promotes macrophage-mediated immune-suppression *in situ* in PDA, we assessed macrophage recruitment and phenotype in both our slowly progressive (KC) and invasive (KPC) models of PDA in the contexts of either Dectin-1 deletion or activation. KC;Dectin-$1^{-/-}$ mice exhibited significantly reduced pancreatic infiltration with $F4/80^+$ and $Arg1^+$ TAMs on IHC analysis (Figure 4a, b). Flow cytometry confirmed a ~50% reduction in the fraction of TAMs in KC;Dectin-$1^{-/-}$ pancreata (Figure 4c). We found a similar decrease in the fraction of TAMs in orthotopic KPC tumors in Dectin-$1^{-/-}$ hosts compared with WT (Figure 4d). Accordingly, analysis of orthotopic KPC tumors using a PCR array suggested reduced expression of diverse inflammatory mediators in tumors in Dectin-$1^{-/-}$ hosts compared with WT (Figure S5d). Moreover, cellular phenotyping experiments indicated that Dectin-1 deletion induced immunogenic reprogramming of TAMs toward M1-like differentiation. Specifically, TAMs infiltrating Dectin-$1^{-/-}$ pancreata expressed elevated MHC II, reduced CD206, and higher TNF-α and iNOS compared with Dectin-$1^{+/+}$ hosts suggesting M1-like programming (Figure 4e–g). By contrast, the prevalence and immune-phenotype of $CD11c^+MHCII^+$ DC was similar in both WT and Dectin-$1^{-/-}$ PDA tumors (Figure S5e, f).

We confirmed that exogenous Dectin-1 ligand administration using d-Zymosan activates Syk signaling in the PDA TME (Figure 4h). Accordingly, *in vivo* Dectin-1 ligation increased the fraction of TAMs in orthotopic KPC tumors (Figure 4i), and upregulated CD206 expression (Figure 4j); however, MHC II expression was not significantly altered (Figure 4k). Similar effects on macrophage programming were seen after *in vivo* treatment with HKCA (not shown). Moreover, adoptive transfer of WT macrophages coincident with PDA tumor challenge in Dectin-$1^{-/-}$ hosts resulted in an accelerated tumor growth rate compared with adoptive transfer of Dectin-$1^{-/-}$ macrophages (Figure 4l).

Dectin-1 signaling suppresses T cell immunogenicity in PDA

Based on the macrophage phenotyping and adoptive transfer experiments and our *in vitro* co-culture data, we postulated that the reprogramming of TAMs resulting from Dectin-1 deletion in PDA leads to enhanced immunogenicity in tumor-entrained T cells. To test this,

we interrogated the T cell phenotype in pancreas-draining lymph nodes in KC vs KC;Dectin-1$^{-/-}$ mice, as well as in orthotopic KPC tumors in WT vs Dectin-1$^{-/-}$ hosts. Consistent with our hypothesis, Dectin-1 deletion in KC mice led to immunogenic reprogramming of tumor-draining CD4^{+} and CD8^{+} T cells, which exhibited upregulated expression of CD44, OX40, and PD-1 indicative of cellular activation (Figure 5a–c). Dectin-1 deletion also increased the CD8:CD4 ratio in tumor draining lymph nodes (Figure 5d). Similarly, Dectin-1 deletion increased the CD8:CD4 ratio in tumor-infiltrating T cells in orthotopic KPC tumors (Figure 5e). Further, CD8^{+} T cells in KPC tumors in Dectin-1$^{-/-}$ hosts exhibited an activated phenotype with high expression of PD-1, T-bet, TNF-α, CD107a, and Granzyme B suggesting enhanced cytotoxic potential compared with orthotopic KPC tumors in WT hosts (Figure 5f). Accordingly, orthotopic administration of KPC cells engineered to express OVA resulted in a markedly higher fraction of tumor-infiltrating OVA Pentamer^{+} cytotoxic T cells in Dectin-1$^{-/-}$ hosts compared with WT (Figure S5g, h). Similarly, PDA-infiltrating CD4^{+} T cells in Dectin-1$^{-/-}$ hosts expressed higher CD44, CD107a, and ICOS and exhibited enhanced Th1 polarization as evidenced by upregulated expression of T-bet and TNF-α (Figure 5g). Collectively, these data indicate enhanced T cell immunogenicity. Notably, consistent with higher T cell activation and PD-1 expression in PDA tumors in Dectin-1$^{-/-}$ mice, combined Dectin-1 deletion + PD-1 blockade trended to offer synergistic protection and further enhanced intra-tumoral Th1 polarization whereas PD-1 blockade had no efficacy in absence of Dectin-1 deletion (Figure 5h, i).

We postulated that exogenous Dectin-1 ligation would induce an immune-suppressive Th2 phenotype and reduce CD8^{+} T cell activation. Accordingly, CD4^{+} T cells harvested from d-Zymosan treated KPC-tumor bearing mice exhibited reduced T-bet and TNF-α expression but higher IL-5, IL-10, and IL-13 expression (Figure S6a). Similarly, CD8^{+} T cells exhibited diminished T-bet and TNF-α expression after Dectin-1 ligation (Figure S6b). Further, *in vivo* macrophage depletion activated PDA-infiltrating CD4^{+} and CD8^{+} T cells exclusively in WT hosts but not in Dectin-1$^{-/-}$ hosts, suggesting that Dectin-1-expressing macrophages drive T cell suppression in PDA (Figure S6c, d).

To definitively test whether tumor-protection in the absence of Dectin-1 signaling is contingent on immunogenic T cell reprogramming, we depleted T cells coincident with orthotopic KPC tumor administration in cohorts of WT and Dectin-1$^{-/-}$ animals. Pan-T cell depletion did not affect PDA growth in WT mice; however, tumor protection was abrogated in Dectin-1$^{-/-}$ cohorts (Figure S6e). Similarly, CD4^{+} and CD8^{+} T cell depletion alone each reversed tumor-protection in Dectin-1$^{-/-}$ mice (Figure S6f, g) but not in WT (not shown). These data suggest that in PDA-bearing WT hosts, T cells are dispensable to outcome; conversely, in the absence of Dectin-1 signaling, T cells are reprogrammed into indispensable mediators of tumor-protection.

Galectin-9 ligates Dectin-1 in PDA

Non-pathogen derived Dectin-1 ligands have not been well-characterized. Therefore, we performed affinity purification-mass spectrometry using the IgG Fc-conjugated Dectin-1 fusion protein coupled to protein G beads to purify putative ligand(s) in KPC tumor extracts.

The proteins co-purified with the Dectin-1 fusion protein were contrasted with proteins purified with protein G beads alone. Affinity purification coupled with mass spectrometry experiments were repeated twice and only proteins that uniquely co-purified with the IgG Fc-conjugated Dectin-1 fusion protein were considered possible candidate Dectin-1 ligands. A total of 19 proteins were identified. Among the co-purified proteins was Galectin-9 (Table S1). Since Galectin-9 is a member of the β-galactoside-binding family of lectins, we hypothesized that Galectin-9 is a sterile ligand for Dectin-1. We assayed for the presence of Galectin-9 in the murine PDA TME and found robust expression of Galectin-9 in diverse PDA-infiltrating myeloid cells and in cancer cells by flow cytometry (Figure 6a, b). We also found modest expression of Galectin-9 in both leukocytes and tumor cells in human PDA whereas Galectin-9 was minimally expressed in leukocytes in PBMC (Figure 6c). We further demonstrated expression of Galectin-9 in PDA-infiltrating leukocytes (13%) and cancer cells (7%) by confocal microscopy (Figure 6d, e). To investigate whether Dectin-1 ligates Galectin-9, protein G-magnetic beads were loaded with the Dectin-1 IgG Fc fusion protein or control IgG Fc. Bead–IgG Fc complexes were incubated with recombinant Galectin-9 and then labeled with a fluorescently-conjugated αGalectin-9 mAb and tested for fluorescence by flow cytometry. We found that the IgG Fc-conjugated Dectin-1 fusion protein avidly ligated Galectin-9 whereas controls failed to elicit a positive signal (Figure 6f). Furthermore, our data suggest that Galectin-9 ligation of Dectin-1 may be competitively inhibited by the well-characterized Dectin-1 ligand d-Zymosan (Figure 6f). Galectin-9 also bound murine (Figure 6g) and human (Figure 6h) Dectin-1 in a dose-dependent manner on ELISA. By contrast, murine Dectin-1 did not avidly bind Galectin-3 or Galectin-4 (Figure 6i). We further confirmed that Galectin-9 binds Dectin-1 *in situ* by precipitating Dectin-1 ligands in pancreatic tissue extract from KC mice and then probing for Galectin-9. Our results indicated Dectin-1–Galectin-9 complex formation (Figure 6j). Given that Galectin-9 binds to polylactosamine epitopes on glycoproteins, we assessed whether Galectin-9 ligates Dectin-1 through a glycan/galectin-9 interaction. To test this, we pretreated the Dectin-1 with PNGaseF, an enzyme that cleaves N-linked glycans, and tested whether this modulated the interaction. We observed no change in the binding between the proteins suggesting glycan-independent binding (Figure 6k). In addition, we pretreated Galectin-9 with high concentrations of lactose, a known inhibitor of galectins, prior to incubation with Dectin-1. Again, no alteration of the Dectin-1/Galectin-9 interaction was observed confirming glycan-independent binding (Figure 6k). To determine whether Galectin-9 is a functional Dectin-1 ligand, we treated WT and Dectin-$1^{-/-}$ macrophages with recombinant Galectin-9 and measured Syk phosphorylation. Galectin-9 activated Syk in a Dectin-1-dependent manner (Figure 6l). Similarly, Galectin-9 induced NF-κB signaling in a HEK293 Dectin-1 reporter cell line[16] in a dose dependent manner (Figure 6m). An irrelevant ligand specific for the C-type lectin receptor Mincle did not activate the Dectin-1 reporter cells (not shown).

Galectin-9 blockade is protective against PDA

Since we found that Galectin-9 activates Dectin-1 in PDA, we postulated that Galectin-9 blockade would protect against tumor progression. We found that serial treatment with a neutralizing Galectin-9 mAb extended survival in mice harboring orthotopic KPC tumors (Figure S7a). Galectin-9 blockade also extended survival after mAb treatment was initiated in mice harboring established orthotopic KPC tumors (Figure S7b). Similarly, elevated

Galectin-9 expression was associated with a trend toward reduced survival in human PDA (Figure S7c). To determine whether Galectin-9 blockade induces tumor regression, mice were implanted subcutaneously with PDA cells and treatment with α-Galectin-9 or isotype was commenced after tumor development. Galectin-9 blockade resulted in substantial tumor regression (Figure S7d). Further, akin to Dectin-1 deletion, combined blockade of Galectin-9 and PD-1 trended to offer synergistic protection against orthotopic PDA (Figure S7e) and resulted in enhanced T cell activation (not shown). Moreover, T cell deletion abrogated the protective effects of Galectin-9 blockade (Figure S7f). By contrast, macrophage depletion was protective against PDA in WT hosts as we have previously reported[13]; however, depleting macrophages accelerated tumor growth in the context of Galectin-9 neutralization (Figure S7f). Further, similar to Dectin-1 deletion, Galectin-9 neutralization was associated with immunogenic reprogramming of TAMs in PDA (Figure S7g). These data suggest that Galectin-9 neutralization leads to macrophage-dependent adaptive anti-tumor immunity. Since Galectin-9-based immunotherapy of orthotopic PDA tumors eventually fails – despite more than doubling median survival – we compared the cellular differentiation and inflammatory infiltrate in early (day 21) versus late (day 42) tumors in mice treated with αGalectin-9. Tumor differentiation, macrophage infiltration, and polarization were similar in early and late tumors (Figure S7h–j). However, $CD8^+$ T cell infiltration was markedly diminished in advanced tumors and $CD8^+$ T cells expressed lower IFN-γ and T-bet (Figure S7k–m).

To determine whether the immune-suppressive T cell program associated with Dectin-1 signaling in the PDA TME was contingent on Galectin-9, we serially blocked Galectin-9 in KPC tumor bearing WT and Dectin-$1^{-/-}$ mice. Galectin-9 neutralization enhanced intra-tumoral T cell activation in PDA in WT hosts. However, Galectin-9 neutralization failed to further enhance $CD4^+$ or $CD8^+$ T cell phenotype in the context of Dectin-1 deletion (Figure S8a, b). Collectively, our data suggests that the Dectin-1 – Galectin-9 axis plays a pivotal role in the education of $CD4^+$ and $CD8^+$ T cells toward immunogenic or tolerogenic phenotypes in PDA, which regulates oncogenic progression (Figure S8c).

Discussion

Pancreatic ductal adenocarcinoma (PDA) is a devastating disease in which the mortality rate approaches the incidence rate[1]. Specifically, PDA is almost invariably associated with a robust inflammatory infiltrate which can have divergent influences on disease progression by either combating cancer growth via antigen-restricted tumoricidal immune responses or by promoting tumor progression via induction of immune suppression[17–19]. For example, $CD8^+$ T cells and Th1-polarized $CD4^+$ T cells mediate tumor protection in murine models of PDA and are associated with prolonged survival in human disease[20]. Conversely, we and others reported that Th2-polarized $CD4^+$ T cells promote PDA progression in mice and intra-tumoral $CD4^+$ Th2 cell infiltrates correlate with reduced survival in human disease[3,20,21]. Similarly, $Foxp3^+$ Tregs facilitate tumor immune escape and shorten survival in PDA[22,23]. Hence, T cell programing influences disease outcome in PDA. However, regulation of the balance between immunogenic and immune-suppressive T cell populations is uncertain. Our data suggest that Dectin-1 signaling plays a critical role in the capacity of macrophages to educate $CD4^+$ and $CD8^+$ T cells toward immunogenic or tolerogenic phenotypes.

Dectin-1 is vital in the innate immune defense against fungal pathogens[24]. Patients with genetic deficiencies in Dectin-1 are at risk for recurrent mucocutaneous fungal infections, such as vulvovaginal candidiasis or onychomycosis[25]. However, unlike their TLR cousins, a definitive role for Dectin-1 in promoting non-pathogen mediated inflammation or oncogenesis is lacking[26]. We previously reported that in the context of chronic liver disease Dectin-1 signaling secondarily protects against liver cancer development by suppressing TLR4 which drives liver fibrosis and increases the associated risk for development of hepatocarcinogenesis[12]. Additional evidence also suggests that in select contexts Dectin-1 activation may bolster anti-tumor immunity. Chiba et al. showed that Dectin-1 expression on antigen presenting cells is critical to NK-mediated killing of tumor cells that overexpress N-glycan structures[27]. Dectin-1 recognition of these tumor cells causes the activation of the IRF5 transcription factor and gene induction necessary for the tumoricidal activity of NK cells. Orally administered β-glucans may be protective in lung and mammary tumor models by ligating Dectin-1 and inducing tumoricidal responses[28]. By contrast, we demonstrate that Dectin-1 critically regulates macrophage phenotype in PDA, which dictates the immunogenic or tolerogenic properties of peritumoral T cells. Moreover, we show that whereas T cells are dispensable in PDA, as T cell deletion does not influence tumor growth, Dectin-1 deletion renders T cells indispensable to tumor protection. These data suggest that targeting Dectin-1 may be an attractive strategy for PDA immunotherapy in experimental therapeutics. We recently reported that activation of Mincle, another C-type lectin receptor, also has pro-tumorigenic properties[13]. However, unlike Dectin-1, Mincle is a well-described death receptor as Mincle ligates byproducts of necroptotic cell death within the PDA TME, including SAP130, leading to expansion of Tregs[13,29]. Of note, we did not find differential Treg expansion as a consequence of Dectin-1 signaling in PDA (not shown).

Interestingly, we found that in addition to Dectin-1 expression on peri-tumoral macrophages and myeloid cells, PDA cells also express Dectin-1. However, the functional implications of Dectin-1 in transformed epithelial cells appear to be inconsequential to tumorigenesis as Dectin-1 ligation or knockdown in PDA cells did not influence their proliferative or inflammatory properties nor did it affect tumor growth *in vivo*. Similarly, Dectin-1 deletion in the inflammatory compartment alone is protective against PDA growth and extends survival. These data were confirmed by our macrophage adoptive transfer experiments. Our finding parallel our previous work investigating TLR4 or TLR9 signaling in PDA, which found that whereas these pattern recognition receptors are highly expressed on tumor cells, receptor ligation does not directly influence tumor progression[3,14].

Beyond elucidating a critical role for Dectin-1 signaling in macrophages in modulating T cell plasticity in the transformed pancreas, one of the most important observations in this study is the discovery that Galectin-9, a lectin with affinity for β-galactosides, is a functional ligand for Dectin-1. Non-pathogen derived ligands for Dectin-1 have not been well-described. Thus, these data may have far-reaching implications to a broader role for Dectin-1 in sterile inflammation and oncogenesis. Galectin-9 has been reputed as an exhaustion ligand for the TIM3 checkpoint receptor on T cells[30]. TIM3 is also expressed on macrophages and dendritic cells[31]. However, the Galectin-9-TIM3 relationship has recently been called into question[32]. Galectin-9 has also recently been shown to bind CD137 where it facilitates receptor complex aggregation, signaling, and functional activity in lymphocytes

and myeloid cells[33]. Hence, Galectin-9 may have a broader role in immune regulation. However, we found that Galectin-9 neutralization only enhanced T cell activation in Dectin-$1^{+/+}$ hosts suggesting that Galectin-9 exerts primary immune-suppressive effects specific to Dectin-1 signaling. Of note, Martinez-Bosch et al. recently reported that Galectin-1 promotes PDA growth via stromal remodeling and hedgehog signaling activation suggesting a role for other Galectins in PDA progression[34]. Additional reports have shown that Galectin-1 contributes to tumor aggressiveness by promoting angiogenesis and T cell apoptosis whereas blockade of Galectin-1 *in vivo* results in tumor rejection via the generation of tumor-specific T cell-mediated responses[35,36]. Conversely, Galectin-3 ligation has been shown to activate tumor-infiltrating lymphocytes and promote anti-tumor immunity[37]. We found that other Galectins did not avidly bind Dectin-1 thus implicating alternate mechanisms.

Our data suggest that, akin to Dectin-1, Galectin-9 would be an attractive target for immunotherapy in PDA. In contrast to our findings, Galectin-9 has been reported to prevent metastases in colon and melanoma models by inhibiting the binding of tumor cells to extracellular matrix components, leading to the prevention of tumor cell migration[38]. There are also important limitations to targeting Dectin-1 or Galectin-9 in PDA as animals do eventually progress based on our survival experiments. These data suggest that Dectin-1 or Galectin-9 targeted immunotherapy would require additional treatments to achieve cure. Indeed, the complex network of immunosuppressive pathways present in tumors are unlikely to be overcome by intervention with a single immune-modulatory agent[39]. Acquired resistance to checkpoint-based immunotherapy in patients with melanoma was associated with defects in the pathways involved in interferon-receptor signaling and in antigen presentation[40]. Relapse after immunotherapy has also been linked to upregulated expression of exhaustion ligands by tumors[41]. Our comparison of day 21 versus day 42 PDA tumors in cohorts of mice treated with α-Galectin-9 suggests that eventually $CD8^+$ T cell expansion and activation fails. It is conceivable that the $CD8^+$ T cells activated by interrupting the Dectin-1 – Galectin-9 axis eventually become exhausted based on reduced IFN-γ and T-bet expression. In fact, our data suggest that combination immunotherapy regimens targeting Dectin-1 or Galectin-9 + PD-1 are likely to have synergistic efficacy, with Dectin-1/Galectin-9 blockade enhancing T cell activation and PD-1 blockade preventing exhaustion via checkpoint receptor ligation. Consistent with our findings, a recent report suggested that durable regression of established tumors in melanoma requires concurrent immunotherapy with four distinct agents which target complementary aspects of innate and adaptive immunity[39]. Thus, the development of therapeutics targeting Dectin-1 signaling will potentially enable immunotherapeutic options in human PDA.

Methods

Animals and In Vivo Models

C57BL/6 (H-2Kb) mice were purchased from Jackson Labs (Bar Harbor, ME) and bred in-house. Dectin-$1^{-/-}$ mice were a gift of Gordon Brown (University of Aberdeen, UK). KC (gift of Dafna Bar-Sagi) and KPC (gift of Mark Philips, both New York University) mice develop pancreatic neoplasia endogenously by expressing mutant *Kras* alone or mutant *Kras*

and *p53*, respectively, in the progenitor cells of the pancreas[42,43]. We previously detailed tumor progression and survival in control KC mice[44]. Dectin-1$^{-/-}$ mice were crossed with KC mice to generate KC;Dectin-1$^{-/-}$ animals. For orthotopic pancreatic tumor challenge, mice were administered intra-pancreatic injections of either Kras^{G12D} PDEC or FC1242 tumor cells derived from KPC mice. Kras^{G12D} PDEC and FC1242 cells were generated as previously described[6,14]. In select experiments we utilized KPC-derived tumor cells (1×10^6) which we engineered to express OVA using pCI-neo-cOVA (gift of Maria Castro; Addgene plasmid # 25097) as we described[44]. Both male and female mice were used but animals were sex- and age-matched in each experiment. For orthotopic tumor experiments, 8–10 week old mice were used. No formal power analyses, randomization, exclusions, or blinding were done. In preparation for intra-pancreatic injection, cells were suspended in PBS with 50% Matrigel (BD Biosciences, Franklin Lakes, NJ) and 1×10^5 tumor cells were injected into the body of the pancreas via laparotomy. Mice were sacrificed 3 weeks later and tumor weight recorded. In select experiments, KPC-derived tumor cells ($5–10\times10^5$) were administered subcutaneously alone or mixed with macrophages (2×10^5). To study the effects of Dectin-1 ligation, mice were administered d-Zymosan (500ug) or HKCA (5×10^7cells; both Invivogen, San Diego, CA) by i.p. injection five times weekly for 8 weeks in endogenous tumor models and for 3 weeks in the orthotopic tumor models. PDEC were harvested from pancreata of KC mice and passaged *in vitro* as previously described[6]. PDEC proliferation was measured using the XTT assay according to the manufacturer's protocol (Roche, Nutley, NJ). In select experiments, cohorts of mice were treated five times weekly with the p-Syk inhibitor Piceatannol (20mg/kg, i.p.; Selleck Chemicals, Houston, TX). Pan-T cells (CD90, T24/31), CD4 T cells (GK1.5), CD8 T cells (53–6.72), and macrophages (F4/80, CI:A3-1, all BioXcell, West Lebanon, NH) were depleted with neutralizing mAbs using regimens we have previously described[13,45]. In other experiments, animals were treated twice weekly with i.p. injection of neutralizing mAbs directed against PD-1 (29F. 1A12, 6mg/kg), or Galectin-9 (RG9-1, 6mg/kg; both BioXCell) or respective isotype controls. Bone marrow chimeric animals were created by irradiating mice (9 Gy) followed by i.v. bone marrow transfer (1×10^7 cells) from non-irradiated donors as we previously described[15]. Chimeric mice were used in experiments 7 weeks later. All animal procedures were approved by the New York University School of Medicine IACUC.

Cellular Harvest and Flow Cytometry

Human or murine single cell suspensions for flow cytometry were prepared as described previously with slight modifications[13]. Briefly, pancreata were placed in cold RPMI 1640 with Collagenase IV (1 mg/mL; Worthington Biochemical, Lakewood, NJ) and DNAse I (2 U/mL; Promega, Madison, WI) and minced with scissors to sub-millimeter pieces. Tissues were then incubated at 37°C for 30 minutes with gentle shaking every 5 minutes. Specimens were passed through a 70μm mesh, and centrifuged at 350g for 5 minutes. The cell pellet was resuspended in cold PBS with 1% FBS. Single cell splenocyte suspensions were prepared as previously described[13]. Cell labeling was performed after blocking FcγRIII/II with an anti-CD16/CD32 mAb (eBioscience, San Diego, CA) by incubating 1×10^6 cells with 1 μg of fluorescently conjugated mAbs directed against murine CD44 (IM7), CD206 (C068C2), PD-1 (29F.1A12), CD3 (17A2), CD4 (RM4-5), CD8 (53-6.7), CD45 (30-F11), CD11b (M1/70), Gr1 (RB6-8C5), CD11c (N418), MHC II (M5/114.15.2), IL-6

(MP5-20F3), IL-5 (TRFK5), IL-10 (JES5-16E3), IFN-γ (XMG1.2), TNFα (MP6-XT22), F4/80 (BM8), ICOS (15F9), OX40 (OX86), CD133 (315-2c11), CD62L(MEL-14), CD107a (1D4B), Galectin-9 (RG9-35; all Biolegend, San Diego, CA), Tbet (eBio4B10), iNOS (CXNFT), IL-13 (eBio13A), Granzyme B (NGZB), FoxP3 (FJK-16s), p-Syk (moch1ct; all eBioscience), Dectin-1 (2A11, Abcam), and Dectin-1 Fc (fc-mdec1a; InvivoGen). Human PDA-infiltrating cells and PBMC were stained with mAbs directed against CD45 (HI30), CD14 (HCD14), CD15 (W6D3), Galectin-9 (9M1-3), and CD11c (3.9; all Biolegend). OVA-restricted $CD8^+$ T cells were identified using an OVA-Pentamer (Proimmune, Oxford, UK). Dead cells were excluded from analysis using zombie yellow (Biolegend). Intracellular cytokine staining was performed using the Fixation/Permeabilization Solution Kit (BD Biosciences) for cytokines, transcription factors, and Granzyme B. Flow cytometry was carried out on the LSR-II flow cytometer (BD Biosciences). Data were analyzed using FlowJo v.10.1 (Treestar, Ashland, OR). BMDM were prepared as previously described[46]. In select experiments IL-12 (0.1 ng/ml; both R&D Systems, Minneapolis, MN), TNF-α (8 pg/ml; Cell Signaling, Beverly, MA), or TGF-β (0.2 ng/ml; Biolegend) were added to day 8 BMDM cultures for 24h. Alternatively, BMDM were cocultured with KPC-derived tumor cells (50:1 ratio).

Histology, Immunohistochemistry, and Microscopy

For histological analysis, pancreatic specimens were fixed with 10% buffered formalin, dehydrated in ethanol, embedded with paraffin, and stained with H&E or Gomori's Trichrome. The fraction of preserved acinar area was calculated as previously described[13]. Pancreatic ductal dysplasia was graded according to established criteria[47]. Immunohistochemistry on frozen or paraffin embedded mouse tissues was performed using antibodies directed against F4/80 (CI:A3-1, Conc: 10μg/ml), Arginase1 (Polyclonal, Conc: 2μg/ml), p-Syk (Polyclonal, Conc: 10μg/ml), Ki67 (Polyclonal, Conc: 3μg/ml), and Dectin-1 (2A11, Conc: 5μg/ml, all Abcam). For paraffin-embedded samples (F4/80, p-Syk, Ki67, Arginase1), samples were dewaxed in ethanol followed by antigen retrieval with 0.01M Sodium Citrate with 0.05% Tween. For frozen specimen (Dectin-1), samples did not undergo antigen retrieval prior to incubation with the primary antibody. Immunofluorescent staining on frozen mouse tissues was performed using antibodies against Dectin-1 (2A11; Conc: 20μg/ml, Abcam), CD45 (30-F11; Conc: 6.25μg/ml, BD Biosciences), CK19 (Troma-III; University of Iowa), CD68 (FA-11, Conc: 5μg/ml, Abcam), Dectin-1 Fc (fc-mdec1a; InvivoGen), Galectin-9 (Polyclonal; Conc: 20μg/ml, Bioss) and DAPI (Vector Labs, Burlingame, CA). Immunofluorescent staining in human tissue was performed using antibodies against Dectin-1 (Polyclonal; Conc: 20μg/ml, Abcam), CD11b (M1/70, Conc: 5μg/ml), Ep-CAM (G8.8; Conc: 5μg/ml, both Biolegend) and DAPI (Vector Labs, Burlingame, CA). Immunofluorescent images were acquired using the Zeiss LSM700 confocal microscope with ZEN 2010 software (Carl Zeiss, Thornwood, New York). All human tissues were collected using an IRB approved protocol and donors of de-identified specimens gave informed consent. Sample sizes for human experiments were not determined based on formal power calculations. Quantifications were performed by assessing 10 high-power fields (HPF; 40X) per slide in a blinded manner.

Western Blotting and RNA Analysis

For protein extraction, tissues were homogenized in ice-cold RIPA buffer. Total protein was quantified using the DC Protein Assay according to the manufacturer's instructions (BioRad, Hercules, CA). Western blotting was performed as previously described with minor modifications[13]. Briefly, 10 % Bis-Tris polyacrylamide gels (NuPage, Invitrogen) were equiloaded with 10–30μg of protein, electrophoresed at 200V, and electrotransferred to PVDF membranes. After blocking with 5% BSA, membranes were probed with primary antibodies to β-actin (8H10D10), p53 (7F5), PLC-γ (polyclonal), p-PLC-γ (polyclonal), Bcl-XL (54H6; all Cell Signaling), JNK (2C6), p-JNK (G9), Smad4 (polyclonal), p16 (polyclonal), c-Myc (9E10), CARD9 (polyclonal), Syk (polyclonal), p-Syk (polyclonal), Rb (C-15; all Cell Signalling), Dectin-1 (polyclonal; Abcam), Galectin-9 (polyclonal), and Dectin-1 Fc (fc-mdec1a; InvivoGen). Blots were developed by ECL (Thermo Scientific, Asheville, NC). RNA extraction was performed using the RNeasy Mini kit (Qiagen, Germantown, MD) as per manufacturer's instructions. For Nanostring analysis, the nCounter mouse inflammation panel was employed using the nCounter Analysis System (both Nanostring, Seattle, Washington).

Enrichment of endogenous Dectin-1 ligands and mass spectroscopy

Cell lysate of KPC-derived tumor cells were prepared and protein was quantified as above. Lysate (2mg) was mixed overnight at 4°C with a human IgG Fc-conjugated Dectin-1 fusion protein (3mg) and protein-G magnet beads (10ml; 10003D, Dynabeads, FisherThermo, Grand Island, NY). Magnet beads were then washed once with 1%NP40 lysis buffer, three times with 0.5M NaCl, and once with H_2O. The affinity purified sample was eluted off the beads by boiling with SDS loading buffer. Samples were reduced with DTT at 57°C for 1 hour and then alkylated with iodoacetamide at 37°C in the dark for 45 minutes (2μl of 0.5M in 100mM ammonium bicarbonate). After alkylation, samples were loaded onto a NuPAGE 4–12% Bis-Tris Gel 1.0 mm (Life Technologies Corporation, Grand Island, NY) and run for 15 minutes at 200 V. The gel was stained using GelCode Blue Stain Reagent (Thermo Scientific, Rockford, IL). The short gel lane was cut into approximately $1mm^3$ pieces. The gel pieces were destained in 1:1 v/v solution of methanol and 100mM ammonium bicarbonate at 4°C with agitation. The destain solution was changed every 15 minutes at least 5 times and until pieces had no visibly blue stain left. Gel pieces were partially dehydrated with an acetonitrile rinse and further dried in a SpeedVac concentrator for 20 minutes. Sequencing grade-modified trypsin (300ng; Promega, Madison, WI) was added to the dried gel pieces. After the trypsin was absorbed, 200μl of 100mM ammonium bicarbonate was added to cover the gel pieces and digestion proceeded overnight on a shaker at 37°C. Peptide extraction was performed by adding a slurry of R2 20μm Poros beads (Life Technologies Corporation) in 5% formic acid; 0.2% trifluoroacetic acid (TFA) to each sample at an volume equal to that of the ammonium bicarbonate. Samples were incubated with agitation at 4°C for 4 hours. The beads were loaded onto equilibrated C18 ziptips (Millipore) using a microcentrifuge for 30 sec at 6000 RPM. Gel pieces were rinsed three times with 0.1% TFA and each rinse was added to the corresponding ziptip followed by microcentrifugation. Extracted poros beads were further washed with 0.5% acetic acid. Peptides were eluted off the beads by addition of 40% acetonitrile in 0.5% acetic acid followed by the addition of 80% acetonitrile in 0.5% acetic acid. The organic solvent was

removed using a SpeedVac concentrator and the samples were reconstituted in 0.5% acetic acid. An aliquot of each sample was loaded onto the EASY spray 50 cm C18 analytical HPLC column with <2μm bead size using the auto sampler of an EASY-nLC 1000 HPLC (ThermoFisher) in solvent A (2% acetonitrile, 0.5% acetic acid). The peptides were gradient eluted directly into a Q Exactive (Thermo Scientific) mass spectrometer using a one hour gradient from 2% to 31% solvent B (95% acetonitrile, 0.5% acetic acid), followed by 10 minutes from 31% to 40% solvent B, and 10 minutes from 40% to 100% solvent B. The Q Exactive mass spectrometer acquired high resolution full MS spectra with a resolution of 70,000, an AGC target of 1×10^6, with a maximum ion time of 120 ms, and scan range of 400 to 1500 m/z. HCD MS/MS spectra were acquired using the following instrument parameters: resolution of 17,500, AGC target of 5×10^4, maximum ion time of 120 ms, one microscan, 2 m/z isolation window, fixed first mass of 150 m/z, and Normalized Collision Energy of 27, dynamic exclusion of 30 seconds. The MS/MS spectra were searched against the Uniprot Mouse database combined with mammalian IgG database using Sequest within Proteome Discoverer (ThermoFisher). The results were filtered using a <1% False Discovery Rate searched against a decoy database and all the proteins with less than two unique peptides were excluded. Proteins identified in the control were subtracted from the proteins identified in the Dectin-1 affinity purification and a shortened list interrogated for potential Dectin-1 ligands.

Analysis of Dectin-1 – Galectin-9 interaction

To investigate if Galectin-9 can bind with Dectin-1, Protein G-magnet beads (2 ml; Dynabeads) were loaded with Dectin-1 IgG Fc (1mg) or control IgG Fc before washing and blocking. Subsequently, beads were incubated with recombinant Galectin-9 (2mg; R&D Systems) for 30 min, washed, and stained with PE-conjugated anti-Galectin-9 (Biolegend, San Diego CA). Galectin-9 specific staining was determined by flow cytometry. To investigate the interaction between Galectin-9 and Dectin-1 by ELISA, plates (Maxisorp, Nunc, St. Louis, MO) were coated with recombinant mouse Galectin-9 (2mg; R&D Systems, Minneapolis, MN), Galectin-3, or Galectin-4 (both 2mg; Biolegend) for 16 hours at 4°C, blocked with 1% BSA/PBS for 1 hour, and incubated with increasing doses of Dectin-1 IgG Fc or control IgG Fc for 2 hours. The Galectin-bound Dectin-1 IgG Fc was detected with anti-IgG-HRP. For affinity precipitation experiments, protein G-beads were loaded with Dectin-1 IgG Fc and were then incubated with the extract of 6 month old KC pancreata. Bead-bound precipitates were resuspended with loading buffer, resolved by SDS-PAGE under reduced conditions for western blotting using mAbs specific for Galectin-9. To determine whether Galectin-9 induces Dectin-1 signaling, the Dectin-1 reporter HEK293 cell line[16] (Invivogen) was treated with recombinant Galectin-9 (1–10μg/ml; R&D Systems), d-Zymosan (1–10μg/ml), or Curdlan (10–100 μg/ml; both Invivogen). Dectin-1 signaling was measured by detection of secreted embryonic alkaline phosphatase. In other experiments, WT and Dectin-$1^{-/-}$ splenic macrophages were treated *in vitro* with recombinant Galectin-9 (10ug/ml). Syk phosphorylation was measured by flow cytometry at 3 hours.

Galectin-9 immunoprecipitation experiments with PNGase F or lactulose treatment

Dectin-1 IgG Fc (8 μg; InvivoGen) was treated with PNGase F (20 μl, ~10,000 units; New England Biolabs) following the company's non-denaturing protocol (37°C, 24 hr). PNGase F treated and untreated Dectin-1 IgG Fc samples (4 μg; InvivoGen) were added to protein G beads (25 μl, Dynabeads Protein G; novex) and the mixtures were incubated at room temperature for 10 min. The beads were washed 2 × with PBS-T (pH 7.4 with 0.02% tween). Recombinant mouse Galectin-9 (4 μg; R&D Systems) was resuspended in PBS-T or a solution of 100 mM lactose in PBS-T. Galectin-9 samples were then incubated with the Dynabead/Dectin-1 IgG Fc complex for 20 min at room temperature. The Dynabeads were then washed 3 × with PBS-T and transferred to a clean tube. Galectin-9 and Dectin-1 IgG Fc were eluted in SDS-PAGE buffer (PBS with 10% BME) by heating at 98°C for 10 min. The samples were then analyzed by SDS-PAGE and stained with Coomassie Blue.

Dectin-1 knockdown

Lentivirus was prepared by infecting 293T cells with the either a Scrambled or shDectin (NM_020008.1-298s1c1) plasmid, Δ8.9CR2 plasmid, and vesicular stomatitis virus glycoprotein plasmid (3:1:4 ratio). Supernatant were collected for 3 days post infection. KPC cells were then infected with supernatant in the presence of polybrene (8 μg/ml) for 12 hours X 2 and selected with puromycin (2 μg/ml). The efficacy of gene knockdown was confirmed by PCR, flow cytometry, and western blotting.

Statistical Analysis

Data is presented as mean +/− standard error. Human RNAseq data and clinical correlations were performed using the UCSC Cancer Genomics Browser (https://genome-cancer.ucsc.edu/)[27]. Survival was measured according to the Kaplan-Meier method. Statistical significance was determined by the Student's *t* test (two-tailed) and the log-rank test using GraphPad Prism 7 (GraphPad Software, La Jolla, CA). P-values <0.05 were considered significant.

Supplementary Material

Refer to Web version on PubMed Central for supplementary material.

Acknowledgments

Grant Support: This work was supported by NCI CA168611 (GM), CA155649 (GM), Department of Defense Peer Reviewed Medical Research Program (GM), Lustgarten Foundation (GM), AACR-PanCan (GM), National Pancreas Foundation (CZ), Panpaphian Association of America (CZ), the Irene and Bernard Schwartz Fellowship in GI Oncology (DD).

This work was supported by grants from the National Pancreas Foundation (CPZ), the Pancreatic Cancer Action Network (GM), the Lustgarten Foundation (GM), and National Institute of Health Awards CA155649 (GM), CA168611 (GM), CA193111 (GM, ATH) and the NYU School of Medicine Office of Therapeutics Alliances. We thank the New York University Langone Medical Center (NYU LMC) Histopathology Core Facility, the NYU LMC Flow Cytometry Core Facility, the NYU LMC Microscopy Core Facility, and the NYU LMC BioRepository Center, each supported in part by the Cancer Center Support Grant P30CA016087 and by grant UL1 TR000038 from the National Center for the Advancement of Translational Science (NCATS).

References

1. Yadav D, Lowenfels AB. The epidemiology of pancreatitis and pancreatic cancer. Gastroenterology. 2013; 144:1252–1261. [PubMed: 23622135]
2. Guerra C, et al. Chronic pancreatitis is essential for induction of pancreatic ductal adenocarcinoma by K-Ras oncogenes in adult mice. Cancer cell. 2007; 11:291–302. [PubMed: 17349585]
3. Ochi A, et al. MyD88 inhibition amplifies dendritic cell capacity to promote pancreatic carcinogenesis via Th2 cells. The Journal of experimental medicine. 2012; 209:1671–1687. [PubMed: 22908323]
4. Zhu Y, et al. CSF1/CSF1R blockade reprograms tumor-infiltrating macrophages and improves response to T-cell checkpoint immunotherapy in pancreatic cancer models. Cancer Res. 2014; 74:5057–5069. [PubMed: 25082815]
5. Connolly MK, et al. Distinct populations of metastases-enabling myeloid cells expand in the liver of mice harboring invasive and preinvasive intra-abdominal tumor. Journal of leukocyte biology. 2010; 87:713–725. [PubMed: 20042467]
6. Pylayeva-Gupta Y, Lee KE, Hajdu CH, Miller G, Bar-Sagi D. Oncogenic Kras-induced GM-CSF production promotes the development of pancreatic neoplasia. Cancer cell. 2012; 21:836–847. [PubMed: 22698407]
7. Bayne LJ, et al. Tumor-derived granulocyte-macrophage colony-stimulating factor regulates myeloid inflammation and T cell immunity in pancreatic cancer. Cancer cell. 2012; 21:822–835. [PubMed: 22698406]
8. Goodridge HS, et al. Activation of the innate immune receptor Dectin-1 upon formation of a 'phagocytic synapse'. Nature. 2011; 472:471–475. [PubMed: 21525931]
9. Taylor PR, et al. Dectin-1 is required for beta-glucan recognition and control of fungal infection. Nature immunology. 2007; 8:31–38. [PubMed: 17159984]
10. Strasser D, et al. Syk kinase-coupled C-type lectin receptors engage protein kinase C-sigma to elicit Card9 adaptor-mediated innate immunity. Immunity. 2012; 36:32–42. [PubMed: 22265677]
11. Gross O, et al. Card9 controls a non-TLR signalling pathway for innate anti-fungal immunity. Nature. 2006; 442:651–656. [PubMed: 16862125]
12. Seifert L, et al. Dectin-1 Regulates Hepatic Fibrosis and Hepatocarcinogenesis by Suppressing TLR4 Signaling Pathways. Cell reports. 2015; 13:1909–1921. [PubMed: 26655905]
13. Seifert L, et al. The necrosome promotes pancreatic oncogenesis via CXCL1 and Mincle-induced immune suppression. Nature. 2016; 532:245–249. [PubMed: 27049944]
14. Zambirinis CP, et al. TLR9 ligation in pancreatic stellate cells promotes tumorigenesis. The Journal of experimental medicine. 2015; 212:2077–2094. [PubMed: 26481685]
15. Ochi A, et al. Toll-like receptor 7 regulates pancreatic carcinogenesis in mice and humans. The Journal of clinical investigation. 2012; 122:4118–4129. [PubMed: 23023703]
16. Walachowski S, Tabouret G, Foucras G. Triggering Dectin-1-Pathway Alone Is Not Sufficient to Induce Cytokine Production by Murine Macrophages. PLoS One. 2016; 11:e0148464. [PubMed: 26840954]
17. Zheng L, Xue J, Jaffee EM, Habtezion A. Role of immune cells and immune-based therapies in pancreatitis and pancreatic ductal adenocarcinoma. Gastroenterology. 2013; 144:1230–1240. [PubMed: 23622132]
18. Clark CE, et al. Dynamics of the immune reaction to pancreatic cancer from inception to invasion. Cancer research. 2007; 67:9518–9527. [PubMed: 17909062]
19. Andren-Sandberg A, Dervenis C, Lowenfels B. Etiologic links between chronic pancreatitis and pancreatic cancer. Scand J Gastroenterol. 1997; 32:97–103. [PubMed: 9051867]
20. Fukunaga A, et al. CD8+ tumor-infiltrating lymphocytes together with CD4+ tumor-infiltrating lymphocytes and dendritic cells improve the prognosis of patients with pancreatic adenocarcinoma. Pancreas. 2004; 28:e26–31. [PubMed: 14707745]
21. De Monte L, et al. Intratumor T helper type 2 cell infiltrate correlates with cancer-associated fibroblast thymic stromal lymphopoietin production and reduced survival in pancreatic cancer. The Journal of experimental medicine. 2011; 208:469–478. [PubMed: 21339327]

22. Hiraoka N, Onozato K, Kosuge T, Hirohashi S. Prevalence of FOXP3+ regulatory T cells increases during the progression of pancreatic ductal adenocarcinoma and its premalignant lesions. Clin Cancer Res. 2006; 12:5423–5434. [PubMed: 17000676]
23. Jiang Y, et al. FOXP3+ lymphocyte density in pancreatic cancer correlates with lymph node metastasis. PloS one. 2014; 9:e106741. [PubMed: 25191901]
24. Vautier S, MacCallum DM, Brown GD. C-type lectin receptors and cytokines in fungal immunity. Cytokine. 2012; 58:89–99. [PubMed: 21924922]
25. Ferwerda B, et al. Human dectin-1 deficiency and mucocutaneous fungal infections. N Engl J Med. 2009; 361:1760–1767. [PubMed: 19864674]
26. Bianchi ME. DAMPs, PAMPs and alarmins: all we need to know about danger. J Leukoc Biol. 2007; 81:1–5.
27. Chiba S, et al. Recognition of tumor cells by Dectin-1 orchestrates innate immune cells for anti-tumor responses. eLife. 2014; 3:e04177. [PubMed: 25149452]
28. Hong F, et al. Mechanism by which orally administered beta-1,3-glucans enhance the tumoricidal activity of antitumor monoclonal antibodies in murine tumor models. Journal of immunology. 2004; 173:797–806.
29. Yamasaki S, et al. Mincle is an ITAM-coupled activating receptor that senses damaged cells. Nature immunology. 2008; 9:1179–1188. [PubMed: 18776906]
30. Zhu C, et al. The Tim-3 ligand galectin-9 negatively regulates T helper type 1 immunity. Nature immunology. 2005; 6:1245–1252. [PubMed: 16286920]
31. Anderson AC, et al. Promotion of tissue inflammation by the immune receptor Tim-3 expressed on innate immune cells. Science. 2007; 318:1141–1143. [PubMed: 18006747]
32. Leitner J, et al. TIM-3 does not act as a receptor for galectin-9. PLoS pathogens. 2013; 9:e1003253. [PubMed: 23555261]
33. Madireddi S, et al. Galectin-9 controls the therapeutic activity of 4-1BB-targeting antibodies. The Journal of experimental medicine. 2014; 211:1433–1448. [PubMed: 24958847]
34. Martinez-Bosch N, et al. Galectin-1 drives pancreatic carcinogenesis through stroma remodeling and Hedgehog signaling activation. Cancer research. 2014; 74:3512–3524. [PubMed: 24812270]
35. Banh A, et al. Tumor galectin-1 mediates tumor growth and metastasis through regulation of T-cell apoptosis. Cancer research. 2011; 71:4423–4431. [PubMed: 21546572]
36. Rubinstein N, et al. Targeted inhibition of galectin-1 gene expression in tumor cells results in heightened T cell-mediated rejection; A potential mechanism of tumor-immune privilege. Cancer cell. 2004; 5:241–251. [PubMed: 15050916]
37. Demotte N, et al. A galectin-3 ligand corrects the impaired function of human CD4 and CD8 tumor-infiltrating lymphocytes and favors tumor rejection in mice. Cancer research. 2010; 70:7476–7488. [PubMed: 20719885]
38. Nobumoto A, et al. Galectin-9 suppresses tumor metastasis by blocking adhesion to endothelium and extracellular matrices. Glycobiology. 2008; 18:735–744. [PubMed: 18579572]
39. Moynihan KD, et al. Eradication of large established tumors in mice by combination immunotherapy that engages innate and adaptive immune responses. Nature medicine. 2016; 22:1402–1410.
40. Zaretsky JM, et al. Mutations Associated with Acquired Resistance to PD-1 Blockade in Melanoma. The New England journal of medicine. 2016; 375:819–829. [PubMed: 27433843]
41. Ansell SM, et al. PD-1 blockade with nivolumab in relapsed or refractory Hodgkin's lymphoma. The New England journal of medicine. 2015; 372:311–319. [PubMed: 25482239]
42. Hingorani SR, et al. Preinvasive and invasive ductal pancreatic cancer and its early detection in the mouse. Cancer Cell. 2003; 4:437–450. [PubMed: 14706336]
43. Hingorani SR, et al. Trp53R172H and KrasG12D cooperate to promote chromosomal instability and widely metastatic pancreatic ductal adenocarcinoma in mice. Cancer Cell. 2005; 7:469–483. [PubMed: 15894267]
44. Daley D, et al. gammadelta T Cells Support Pancreatic Oncogenesis by Restraining alphabeta T Cell Activation. Cell. 2016; 166:1485–1499. [PubMed: 27569912]

45. Bedrosian AS, et al. Dendritic cells promote pancreatic viability in mice with acute pancreatitis. Gastroenterology. 2011; 141:1915–1926. e1911–1914. [PubMed: 21801698]

46. Greco SH, et al. Mincle suppresses Toll-like receptor 4 activation. Journal of leukocyte biology. 2016; 100:185–194. [PubMed: 26747838]

47. Hruban RH, et al. Pancreatic intraepithelial neoplasia: a new nomenclature and classification system for pancreatic duct lesions. The American journal of surgical pathology. 2001; 25:579–586. [PubMed: 11342768]

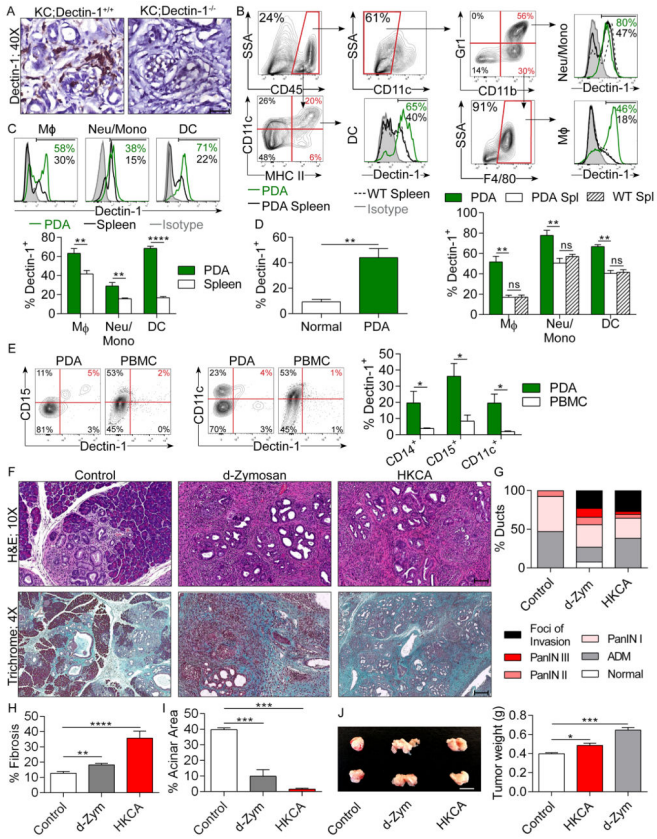

Figure 1. High Dectin-1 expression in mouse and human PDA and Dectin-1 ligation accelerates PDA progression

(a) Frozen sections of 6 month-old KC;Dectin-1$^{+/+}$ and KC; Dectin-1$^{-/-}$ pancreata were tested for expression of Dectin-1 by IHC (scale bar = 100μm). **(b)** PDA-infiltrating and splenic leukocytes from KC and aged-matched WT mice were tested for expression of Dectin-1 in CD11c^{-}Gr1^{-}CD11b^{+}F4/80^{+} macrophages, Gr1^{+}CD11b^{+} neutrophils and inflammatory monocytes, and CD11c^{+}MHCII^{+} dendritic cells. Representative contour plots and quantitative data from 5 mice are shown. **(c)** PDA-infiltrating and splenic leukocytes from mice bearing KPC-derived tumors were tested for expression of Dectin-1 compared with isotype control in CD11c^{-}Gr1^{-}CD11b^{+}F4/80^{+} macrophages, Gr1^{+}CD11b^{+} neutrophils and inflammatory monocytes, and CD11c^{+}MHCII^{+} dendritic cells. Representative contour plots and quantitative data from 5 mice are shown. Murine flow cytometry experiments were repeated more than 3 times. **(d)** Dectin-1 expression was tested by flow cytometry in macrophages from normal pancreas compared with macrophages infiltrating orthotopic PDA tumors (n=5/group). **(e)** Human PDA-infiltrating and PBMC-derived CD14^{+}, CD15^{+}, and CD11c^{+} cells were tested for expression of Dectin-1. Representative contour plots (CD15, CD11c) and quantitative data from 5 PDA patients are shown. **(f–i)** Six week-old KC mice were treated with the Dectin-1 ligands d-Zymosan, HKCA, or vehicle for 8 weeks before sacrifice (n=5/group). (f) Representative H&E (scale bar = 100μm) and Trichrome (scale bar = 200μm) stained sections are shown. (g) The percentage of ducts exhibiting normal morphology, ADM, graded PanIN lesions, or foci of invasive cancer are shown. (h) The percentage of pancreatic area occupied by fibrotic tissues was calculated based on trichrome

staining. (i) The percentage of pancreatic area occupied by normal acinar structures was calculated. **(j)** WT mice were administered orthotopic KPC-derived tumor cells and serially treated with the Dectin-1 ligands d-Zymosan or HKCA or vehicle control. Animals were sacrificed at 3 weeks and pancreas weights measured. Representative gross images of pancreatic tumors and quantitative data are shown (n=5/group; scale bar = 1cm; *p<0.05; **p<0.01; ***p<0.001; ****p<0.0001).

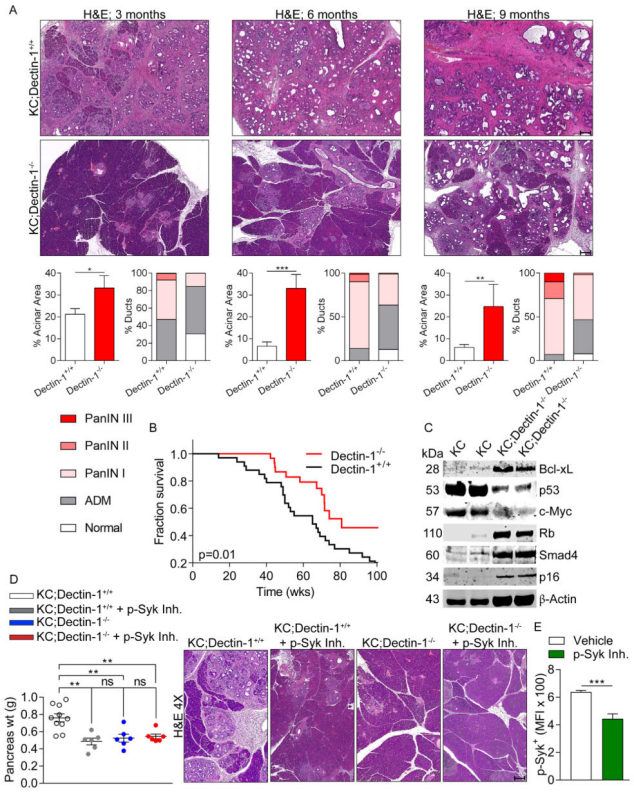

Figure 2. Dectin-1 deletion or blockade is protective against PDA

(a) KC;Dectin-$1^{+/+}$ (n=10) and KC;Dectin-$1^{-/-}$ (n=6) mice were sacrificed at 3, 6, or 9 months of life. Representative H&E-stained sections are shown, the percentage of pancreatic area occupied by intact acinar structures, and the fractions of ductal structures exhibiting normal morphology, acino-ductal metaplasia (ADM), or graded PanIN I-III lesions were calculated (scale bar = 200μm). **(b)** Kaplan-Meier survival analysis was performed comparing KC;Dectin-$1^{+/+}$ (n=29) and KC;Dectin-$1^{-/-}$ (n=41) mice (p=0.01). **(c)** Whole pancreas lysate from 3 month-old KC;Dectin-$1^{+/+}$ and KC;Dectin-$1^{-/-}$ mice were assayed for expression of select oncogenic and tumor suppressor genes. **(d)** Six week-old KC;Dectin-$1^{+/+}$ and KC;Dectin-$1^{-/-}$ mice were serially treated with the p-Syk inhibitor Piceatannol or vehicle for 8 weeks before sacrifice (n=5–10/group). Pancreas weights were measured and representative H&E-stained sections are shown (scale bar = 200μm). Each point represents data from a single mouse. **(e)** WT mice bearing orthotopic PDA were serially treated with the p-Syk inhibitor Piceatannol or vehicle for 3 weeks. Tumor-infiltrating APC were harvested and tested for p-Syk expression by flow cytometry. Median fluorescence index (MFI) is shown (n=5/group; *p<0.05; **p<0.01; ***p<0.001).

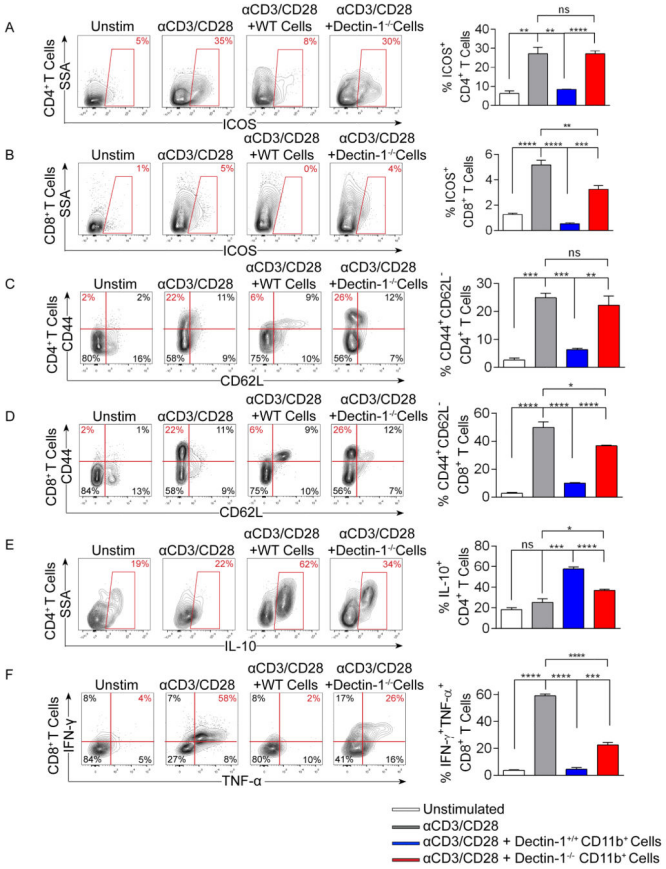

Figure 3. Dectin-1$^{-/-}$ PDA-infiltrating monocytic cells exhibit diminished T cell suppressive properties

Naïve CD4^{+} or CD8^{+} splenic T cells were either unstimulated, stimulated with αCD3/αCD28 alone or in co-culture with PDA-infiltrating CD11b^{+} cells harvested from orthotopic KPC tumors in WT or Dectin-1$^{-/-}$ hosts. CD4^{+} and CD8^{+} T cell activation, respectively, were determined at 72h by **(a, b)** ICOS expression, **(c, d)** the fraction of cells exhibiting the CD62L^{-}CD44^{+} phenotype, **(e)** CD4^{+} T cell expression of IL-10, and **(f)** CD8^{+} T cell co-expression of IFN-γ and TNF-α. Experiments were performed in quadruplicate and repeated 3 times (*p<0.05; **p<0.01; ***p<0.001; ****p<0.0001).

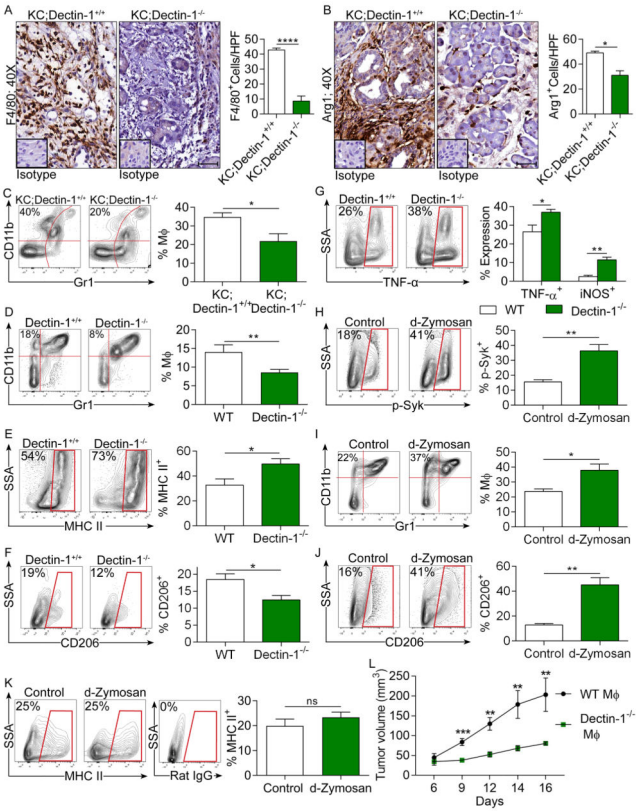

Figure 4. Dectin-1 signaling regulates macrophage infiltration and phenotype in PDA

(a–c) Six month-old KC;Dectin-$1^{+/+}$ and KC;Dectin-$1^{-/-}$ mice were tested for (a) $F4/80^+$ and (b) $Arg1^+$ macrophage infiltration by IHC (n=5/group) (scale bar = 100μm). (c) The fraction of $CD11c^-Gr1^-CD11b^+F4/80^+$ macrophages in the pancreata of three-month old KC;Dectin-$1^{+/+}$ and KC;Dectin-$1^{-/-}$ mice was determined by flow cytometry (n=5/group). **(d–g)** WT and Dectin-$1^{-/-}$ mice were challenged with orthotopic KPC-derived PDA tumors. (d) $CD11c^-Gr1^-CD11b^+F4/80^+$ macrophage infiltration was determined on day 21 by flow cytometry. (e) PDA-infiltrating macrophages were gated and tested for expression of MHC II, (f) CD206, (g) TNF-α, and iNOS (n=5/group). **(h–k)** WT mice were implanted with orthotopic KPC tumors and serially treated with the Dectin-1 specific ligand d-Zymosan or vehicle. (h) Dectin-1 activation was confirmed by upregulation of p-Syk expression in PDA-infiltrating macrophages in d-Zymosan-treated compared with vehicle-treated mice. (i) The fraction of tumor-infiltrating macrophages was determined by flow cytometry on day 21. (j) PDA-infiltrating macrophages were gated and tested for expression of CD206 and (k) MHC II. Representative contour plots and quantitative data are shown (n=5/group). Experiments were repeated more than 3 times with similar results. **(l)** Dectin-$1^{-/-}$ mice were subcutaneously implanted with KPC-derived PDA tumor cells admixed with WT or Dectin-$1^{-/-}$ macrophages. Tumor volume was recorded at serial intervals. This experiment was repeated twice with similar results (n=4/group; *p<0.05; **p<0.01; ****p<0.0001).

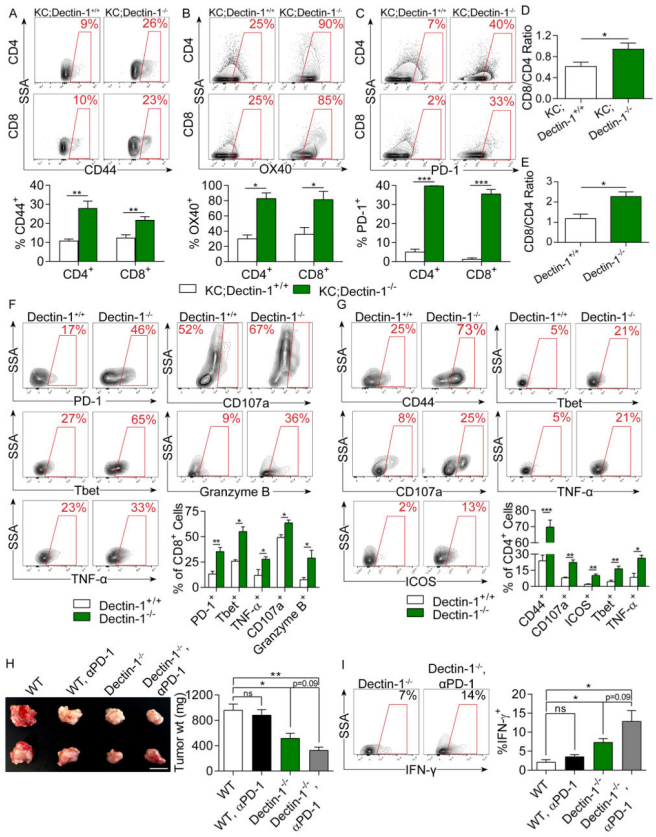

Figure 5. Dectin-1 signaling prevents immunogenic T cell differentiation in PDA

(a–d) The inferior pancreas-draining lymph node in 6 month-old KC;Dectin-1$^{+/+}$ and KC;Dectin-1$^{-/-}$ mice was assayed for (a) CD44, (b) Ox40, and (c) PD-1 expression in CD4^{+} and CD8^{+} T cells, and (d) the CD8^{+}:CD4^{+} T cell ratio. Representative contour plots and quantitative data are shown (n=5/group). **(e–g)** WT and Dectin-1$^{-/-}$ mice were challenged with orthotopic KPC tumors. (e) The CD8^{+}:CD4^{+} ratio was determined on day 21 by flow cytometry. (f) PDA-infiltrating CD8^{+} T cell expression of PD-1, T-bet, TNF-α, CD107a, and Granzyme B were determined by flow cytometry. (g) PDA-infiltrating CD4^{+} T cell expression of CD44, CD107a, ICOS, T-bet, and TNF-α were determined by flow cytometry (n=5/group). (**h, i**) WT and Dectin-1$^{-/-}$ mice were challenged with orthotopic KPC tumors. Cohorts were additionally treated with αPD-1 or isotype control. (h) Tumor weights were measured on Day 21 and (i) the fraction of CD4^{+} T cells expressing IFN-γ was determined by flow cytometry n=5/group. All experiments were repeated at least twice (*p<0.05, **p<0.01, ***p<0.001).

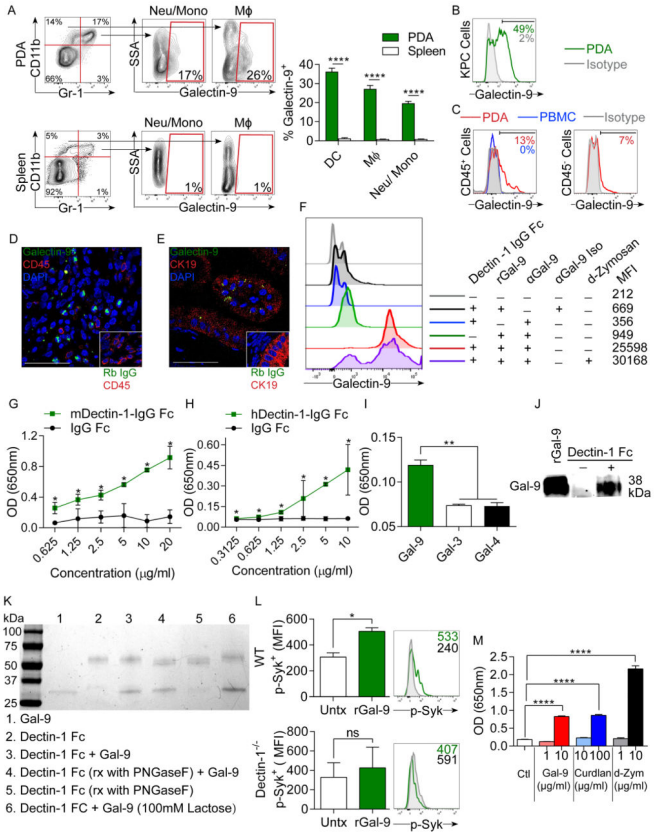

Figure 6. Galectin-9 is a novel Dectin-1 ligand in PDA

(a) PDA-infiltrating and splenic $Gr1^{+}CD11b^{+}$ neutrophils and inflammatory monocytes, $CD11c^{-}Gr1^{-}CD11b^{+}F4/80^{+}$ macrophages, and $CD11c^{+}MHCII^{+}$ DC from mice harboring orthotopic KPC tumors were gated by flow cytometry and tested for expression of Galectin-9. Gates are based on respective isotype control (not shown). Representative contour plots and quantitative data from 5 mice are shown. **(b)** $CD45^{-}CD133^{+}$ pancreatic cancer cells from orthotopic KPC tumors were gated by flow cytometry and tested for expression of Galectin-9 compared with isotype control. Representative data from >3 experiments is shown. **(c)** $CD45^{+}$ and $CD45^{-}$ cells from human PDA tumor tissue were tested for expression of Galectin-9 compared with PBMC. Representative data from one of three patients are shown. **(d)** Frozen sections of orthotopic KPC-derived pancreatic tumors were co-stained for CD45 and Galectin-9 or isotype control and imaged by confocal microscopy. Representative images are shown (scale bar = 50μm). **(e)** Frozen sections of orthotopic KPC-derived pancreatic tumors were co-stained for CK19 and Galectin-9 or isotype control and imaged by confocal microscopy. Representative images are shown (scale bar = 50μm). **(f)** Protein G-magnetic beads were loaded with the Dectin-1 IgG Fc fusion protein. After blocking, the bead–IgG Fc complexes were incubated with recombinant Galectin-9 and then stained with fluorescently-conjugated anti-Galectin-9 and tested for fluorescence by flow cytometry. Controls included: unstained beads, bead–IgG Fc complexes + recombinant Galectin-9 + fluorescently-conjugated isotype antibody, bead–IgG Fc complexes + fluorescently-conjugated anti-Galectin-9, beads without Dectin-1 IgG Fc incubated with recombinant Galectin-9 + fluorescently-conjugated anti-Galectin-9. To test

for competitive inhibition of Galectin-9 binding with a well-characterized Dectin-1 ligand, the bead–IgG Fc complexes were incubated with recombinant Galectin-9 together with d-Zymosan and then stained with fluorescently-conjugated anti-Galectin-9. This assay was repeated twice with similar results. **(g, h)** Galectin-9 coated ELISA plates were incubated with increasing doses of (g) murine or (h) human Dectin-1 IgG Fc or control IgG Fc. The Galectin-9-bound Dectin-1 IgG Fc was detected with anti-IgG-HRP. Averages of triplicates are shown. ELISA assays was repeated twice with similar results. **(i)** Galectin-3, Galectin-4, and Galectin-9 coated ELISA plates were incubated with Dectin-1 IgG Fc or control IgG Fc (2.5μg/ml) in parallel. The Galectin-bound Dectin-1 IgG Fc was detected with anti-IgG-HRP. Averages of triplicates are shown. **(j)** We precipitated Dectin-1 ligands in pancreatic tissue extract from 6 month-old KC mice using the Dectin-1 IgG Fc or control IgG Fc and then probed for Galectin-9 by western blotting. Recombinant Galectin-9 was used as a positive control. This assay was repeated twice with similar results. **(k)** Dectin-1 IgG Fc was treated with either buffer or PNGase F, loaded onto Protein G beads and incubated with recombinant mouse Galectin-9 pre-incubated with 100 mM lactose or buffer. Treated and control samples were analyzed by SDS-PAGE and gels were stained with Coomassie Blue. This experiment was repeated twice with similar results. **(l)** WT and Dectin-$1^{-/-}$ macrophages were treated with Galectin-9 (10ug/ml) for 3 hours. Syk phosphorylation was determined by flow cytometry compared with isotype control. Representative histogram overlays and quantitative data from 5 separate experiments are shown. **(m)** Dectin-1 reporter HEK293 cells were untreated or treated low and high doses of Galectin-9 or well-characterized Dectin-1 ligands Curdlan and d-Zymosan. Dectin-1 activation was measured by detection of secreted embryonic alkaline phosphatase. This assay was performed in triplicate (*$p<0.05$; **$p<0.01$; ****$p<0.0001$).